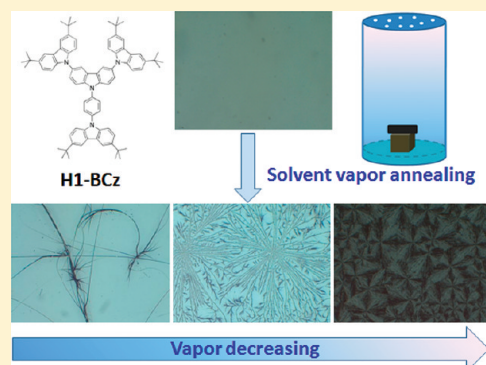


Self-Assembly of Carbazole-Based Dendrimers by Solvent Vapor Annealing: From Fibers to Spherulites

Zicheng Ding, Rubo Xing, Lidong Zheng, Yue Sun, Xingdong Wang, Junqiao Ding, Lixiang Wang, and Yanchun Han*

State Key Laboratory of Polymer Physics and Chemistry, Changchun Institute of Applied Chemistry, Chinese Academy of Sciences and Graduate University of the Chinese Academy of Sciences, 5625 Renmin Street, Changchun 130022, P. R. China

ABSTRACT: The self-assembly behavior of H1-BCz, a first-generation dendrimer with phenyl-carbazole as core and carbazole as dendrons, was systematically studied by solvent-vapor annealing. The morphologies of spin-coated H1-BCz film on various substrates changed from giant crystalline fibers of several millimeters to spherulites with a decrease in tetrahydrofuran vapor pressure. At high vapor pressure, dewetting easily took place in the amorphous films, and single fibers or fiber clusters formed. The fibers grew from nuclei formed at the place where it does not dewet. The fibers grew larger by continuous nucleation and growth at the growth front of the fiber until all the substance on the substrate was consumed. As the vapor pressure decreased, dewetting did not so easily happen, and fibers packed more tightly and spherulites were obtained. Through characterization of the crystals and films, we speculate that 3D H1-BCz crystal formed by overlapping 2D lamellar structure. The $\pi-\pi$ interactions and van der Waals interactions among H1-BCz molecules and solvent may be the main force driving the self-assembly of H1-BCz.



1. INTRODUCTION

Dendrimers have attracted much attention in the areas of catalysts, biomedicine, and molecular electronics applications in past decades because of their unique three-dimensional dendritic structures and chemistry and physical properties.^{1–5} By properly designing and synthesizing, such as incorporating different cores or changing the dendrons or surface groups, the molecular structures can be modified, and the properties can also be tuned. More importantly, the molecular diversity of dendrimers provides an effective way to change the interactions among dendrimers, solvents, and substrates; thus, hierarchical supramolecular structures with higher complexity and promising properties can be obtained by self-assembly of dendrimers.

π -Conjugated small molecules and polymers have been widely used in optical and electronic devices for their special optical and electronic properties. Many π -conjugated dendrimers have been synthesized and found applications in optoelectronic devices, such as organic light-emitting diodes (OLEDs), organic thin-film transistors (OTFTs), and organic photovoltaic cells (OPVs). The optical and electronic properties of the films and the performance of the devices are highly influenced by the condensed structures of the dendrimers. The self-assembly behaviors of these rigid shape-persistent dendrimers were also investigated. Moore et al. studied the aggregation of phenylacetylene dendrimer in solution, which was directed by face-to-face $\pi-\pi$ interactions between aromatic rings.^{6,7} Müllen et al. have reported that the polyphenylene dendrimers can self-assemble into nanowires and other aggregation structures by controlling the interactions

among molecules, solvents, and substrates.^{8–11} Recently, Advincula et al. have synthesized and investigated the supramolecular assembly behavior and nanostructures of thiophene dendrimers on mica and graphite substrates.^{12,13}

Carbazole is a conjugated unit that possesses good hole-transport ability and can harvest and transfer energy efficiently.¹⁴ Carbazole derivatives have been widely used in organic optical-electronic devices. Carbazole-based small molecules have found applications in electroluminescence devices as hole-transporting and emitting layers for their good thermal stability and attractive optoelectronic performance.¹⁵ Poly(*N*-vinylcarbazole) and its derivatives have been widely used in electrophotographic materials, photorefractive materials, and light-emitting materials.^{16,17} Recently, carbazole-based compounds for OPVs and OFETs have been developed and gained much advance. The carbazole-nevinylene oligomers,^{18,19} indolo[3,2-*b*]carbazole derivatives,^{20–22} and poly(2,7-carbazole) derivatives²³ have been used in OTFTs. The performance of the devices, such as the carrier mobility, is highly dependent on the ordering of the molecules in the fibers or crystalline films. Compared with the amorphous films, the high ordering crystalline forms of the compounds always lead to higher-performance devices. The carbazole-based dendrimers with proper energy level have also been designed and synthesized as host materials or light-emitting materials for high-performance

Received: May 16, 2011

Revised: November 28, 2011

Published: November 28, 2011

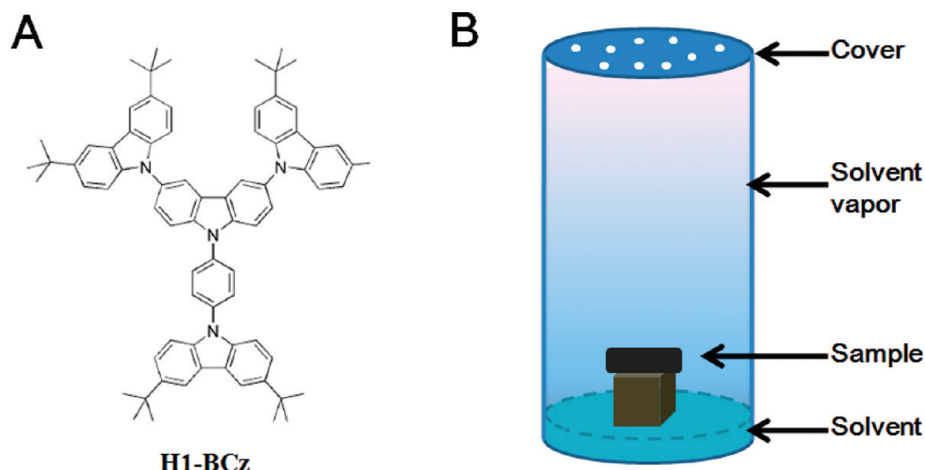


Figure 1. (A) Molecular structure of carbazole-based dendrimer H1-BCz. (B) The schematic of the solvent-vapor induced self-assembly set.

electrophosphorescent devices.^{24–28} But the self-assembly behavior of carbazole-based dendrimers is rarely reported. Because carbazole dendrons are not effectively conjugated to the core through 3,6,9-carbazole linkages, the molecular structure of the carbazole dendrimer is twisted and nonplanar. The desired carbazole-based dendrimers used in OLEDs are amorphous and not easily crystallize with high thermal stability.

In this paper, we show that the as-spun amorphous film of carbazole-based conjugated dendrimer H1-BCz on various substrates can self-assemble into crystalline fibers by exposing the sample to tetrahydrofuran vapor, though H1-BCz is thermally stable with a high glass transition temperature and decomposition temperature.²⁷ The density of the crystalline fibers can be controlled by varying the solvent vapor pressure. As the vapor pressure decreases, the density of the fiber increases, from a single fiber at high vapor pressure to spherulites with crowded packing at low vapor pressure. Through *in situ* observation of the fiber growth process, we find that the morphologies of the dendrimer fibers depend on the nucleation and growth process of the fibers, which are influenced by the dewetting process of the thin film under different vapor pressures. During the self-assembly process, the interactions among the dendrimer molecules and the solvent may be the dominating factor. The properties of the substrates have little effect on the fiber-growth process.

2. EXPERIMENTAL SECTION

2.1. Materials. The carbazole-based dendrimer H1-BCz (Figure 1(A)) was synthesized as shown in ref 27. The solvents tetrahydrofuran (THF), dichloromethane (CH_2Cl_2), and chlorobenzene were purchased from Beijing Chemical Reagent Co. Ltd., China, and were purified before used. The mica substrates were freshly cleaved when used. The glass and silicon substrates were cleaned in a piranha solution (70/30 v/v of concentrated H_2SO_4 and 30% H_2O_2) at 70 °C for 30 min, thoroughly rinsed with deionized water, and dried under nitrogen blow.

2.2. Sample Preparation. H1-BCz was dissolved in chlorobenzene with a concentration of 10 mg/mL, and the solution was put in a dark and vibrationless environment for 24 h at room temperature to obtain homogeneous samples. Before fabricating films, the solution was filtered using a 0.22 μm PTFE filter. Amorphous films with a thickness of 40 nm were fabricated by spin-coating H1-BCz solution from chlorobenzene onto

precleaned substrates. The films were put into a vacuum oven for 24 h to remove the residual solvent. Assemblies of the dendrimers were prepared by putting the amorphous films in a nearly closed glass container (3 cm in diameter and 20 cm in length) with preadded 10 mL of THF solvent to create a saturated solvent environment. The schematic of the self-assembly process is shown in Figure 1B. For the time-resolved, *in situ* observation of the self-assembly process, the container was 4 cm in diameter and 2.5 cm in height with a transparent glass cover with 50 μL of preadded THF. TEM samples were made by exposing the films fabricated on glass substrates in a HF solvent environment for 30 s, and then the films were floated onto the water surface. Pieces of the dendrimer film were then picked up from the deionized water surface onto copper mesh and dried in a vacuum oven for 24 h.

2.3. Characterization. The morphologies of the amorphous films and assemblies of H1-BCz dendrimers were observed by optical microscopy (Zeiss Axio Imager A2m, Carl Zeiss, Germany). The surface morphologies of the films were investigated by atomic force microscopy (AFM) and transmission electron microscopy (TEM). AFM characterization was performed in tapping mode using a SPA300HV with a SPI3800N controller (Seiko Instruments, Inc., Japan). A silicon microcantilever (spring constant 2 N/m and resonance frequency \sim 70 kHz, Olympus Co., Japan) with an etched conical tip was used for the scan. TEM experiments were performed on a TEM-1011 (JEOL Co., Japan) with an accelerating voltage of 100 kV.

Grazing incidence wide-angle X-ray diffraction was applied to determine the structural properties of assembled thin films on SiO_x substrates. All measurements were performed with a diffractometer D8 Discover (Bruker, Germany) ($\lambda = 1.54 \text{ \AA}$). A fixed grazing incidence angle of 0.2° was used to reduce the scattering from the substrates.

The UV-vis absorption spectra were recorded using a Lambda 750 spectrometer (Perkin-Elmer, Wellesley, MA) with 5.0 nm slit, and the PL spectra were recorded using a Perkin-Elmer LS 50B spectrofluorometer. The concentration of the H1-BCz solution in CH_2Cl_2 for the UV-vis absorption spectra and PL spectra was $1 \times 10^{-5} \text{ M}$. The amorphous films and crystallization films were fabricated on quartz substrates.

3. RESULTS AND DISCUSSION

The effect of the solvent vapor pressure on the morphology evolution of the amorphous dendrimer films is discussed in

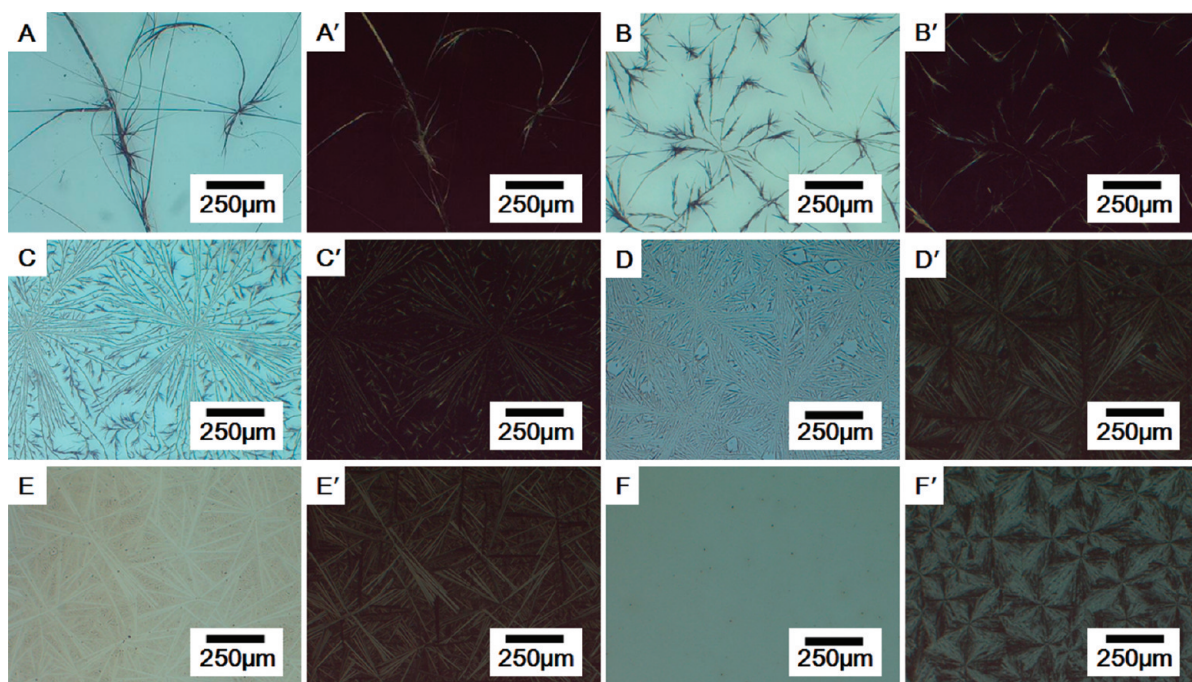


Figure 2. The optical images of the self-assembled H1-BCz fibers formed on glass substrates by exposing the spin-coated films to THF vapor for 16 h with different vapor pressures. The distances between the sample position and the solvent liquid surface are (A) 0.6, (B) 2.6, (C) 3, (D) 3.8, (E) 5.8, and (F) 7.4 cm. A', B', C', D', E', and F' are the polarized images of A, B, C, D, E, and F, respectively.

section 3.1. In section 3.2, the growing process of the fibers is observed, and the influence of the dewetting process on the morphology of the fibers is discussed. Last, we give the probable self-assembly mechanism of H1-BCz dendrimer in section 3.3.

3.1. From Fibers to Spherulites: The Effect of the Solvent Vapor Pressure. The rearrangement of small molecules and polymers can take place by solvent vapor annealing, which has been demonstrated by several groups.^{29–32} The subsequent self-assembly film performs different behaviors from the as-cast films for the different morphologies. The vapor pressure has an effect on the self-assembly morphology. Lu et al. have grown fullerene nanorods with different shapes and sizes in a conjugated polymer film by changing the vapor pressure.³³ Crossland et al. have proved that the crystalline morphology of P3HT can be systematically controlled by precisely controlling the nucleation density and crystal growth conditions in different vapor pressures of carbon disulfide.³⁴ The effect of the solvent vapor pressure on the morphology evolution of the H1-BCz dendrimer films is discussed.

When the distance between the position of the sample and the surface of the liquid solvent changed, the self-assembly morphology varied. When the sample was close to the solvent surface, random distributed single fibers or fiber clusters formed, as shown in Figure 2A. The growth direction of the fibers is with random variation, and the length of the fibers can reach several millimeters. As the distance between the sample position and the solvent surface increased, ring-shaped dendrites consisting of fibers formed. All the fibers originate from ring centers and grow outward, forming their own boundary when fibers from neighboring ring meet together (Figure 2B–E). As the distance becomes much larger, the fibers grow more straightly and pack more tightly. At last, Maltese cross patterns were viewed under polarized light, which means that the spherulites formed (Figure 2F'). The unobvious spherulites in optical microscopy

images (Figure 2F) may be due to the low contrast in unpolarized light.

The AFM and TEM images in Figures 3 and 4 show a more detailed structure image of the self-assembly morphology. The individual fibers are connected by numerous thinner fibers, and there are cracks along the fiber growth direction (Figure 3A and A'). As the distance increases, more and more thin fibers pack together, the fibers at the edge branch off, and the substrate is gradually covered (Figure 3C, C', D, and D'). When the spherulites formed, the whole substrate was covered by the fibers. The fibers with different growth directions pack together, and boundaries form (Figure 3F). The morphology images investigated by TEM in Figure 4 are similar to AFM. Diffraction spots observed for the fibers formed at the lower position, and the diffraction arc for the spherulites formed at the higher position (Figure 4). The electron diffraction (ED) patterns for the fibers and spherulites show that the H1-BCz molecules pack in an orderly manner after self-assembly. Through solvent vapor annealing, H1-BCz molecules in the amorphous films can rearrange and crystallize into more ordered structures.

The different self-assembly morphologies at different positions may be attributed to the different vapor pressures. As the distance between the sample and the surface of the solvent increases, the solvent vapor decreases.³³ We explain the different densities of the fiber at different vapor pressures from two aspects. At high vapor pressure, the naked area decreases as the vapor pressure decreases during the same time period (Figure 2A–E). It indicates that the dewetting does not easily happen at lower vapor pressure. In addition, there are more fibers formed on the substrates as the vapor pressure decreases. For the fibers only formed in the area where the films covered, the density of the fibers per area will increase and the fibers will pack more tightly as the vapor pressure decreases. The relationship between dewetting and fiber growth will be further investigated in the next section.

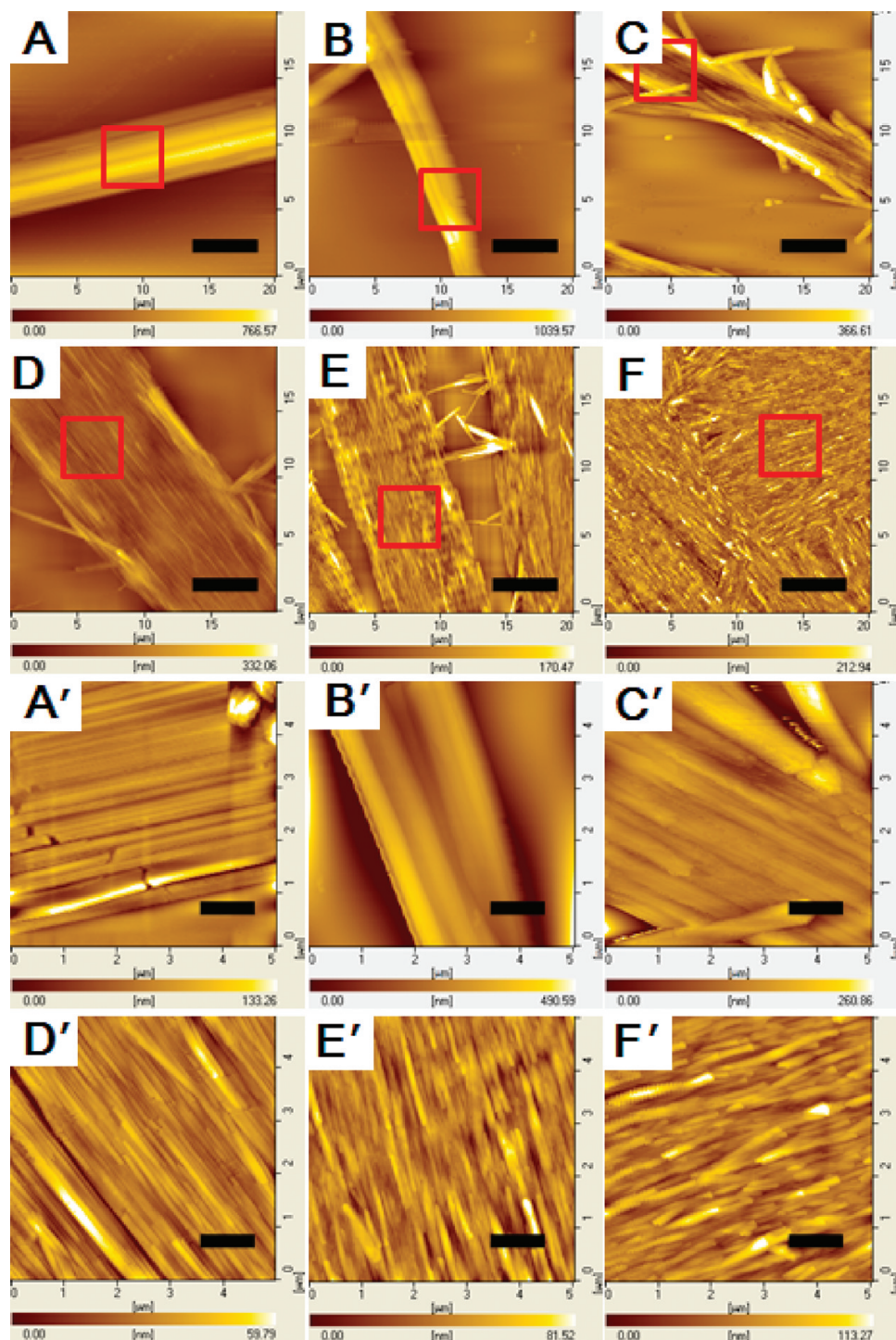


Figure 3. The AFM height images of the self-assembled H1-BCz fibers formed on glass substrates by exposing the spin-coated films to THF vapor for 16 h with different vapor pressures. The distances between the sample position and the solvent liquid surface are (A) 0.6, (B) 2, (C) 3.8, (D) 5.8, (E) 7.4, and (F) 9.4 cm. A', B', C', D', E', and F' are the magnified images of selected areas in A, B, C, D, E, and F, respectively. The scale bar in A–F is 5 μm . The scale bar in A'–F' is 1 μm .

At low vapor pressure when the dewetting of the film does not take place, spherulites form in the swollen film with a high degree of supercooling (Figure 2F, F').³⁵ The size and density of the spherulites also could be controlled in our experiment by changing the solvent vapor pressure, which is similar to the P3HT spherulites under CS₂ vapor.³⁴

3.2. The Time-Resolved Self-Assembly Process of Fibers.

To investigate the whole self-assembly process of H1-BCz, the growth process of the fibers was recorded by the in situ observation of the solvent-vapor annealing process using an optical microscope. Figure 5A shows that the as-spun film of H1-BCz from chlorobenzene solution is amorphous and smooth.

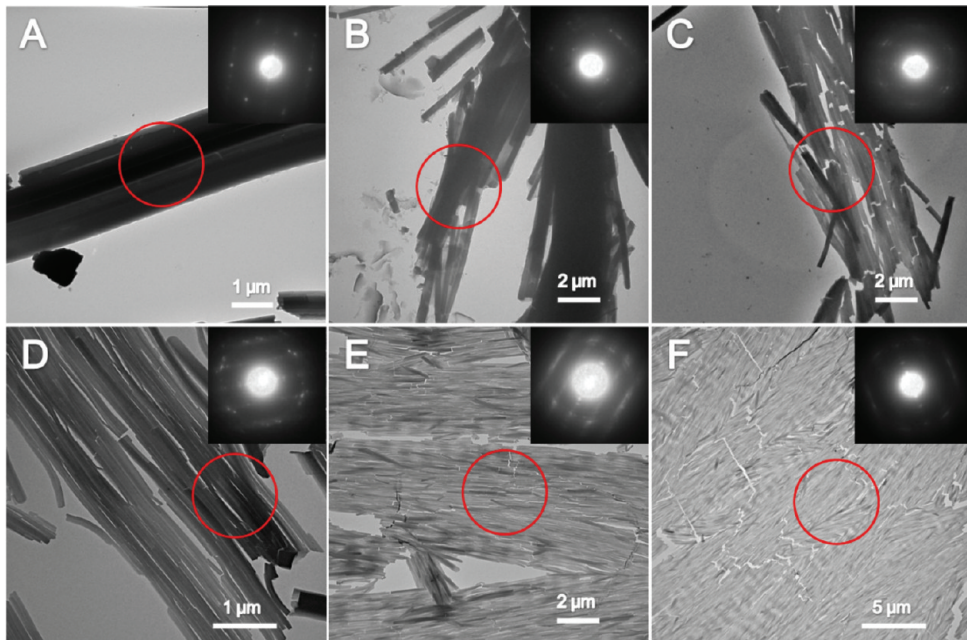


Figure 4. The TEM images of the self-assembled H1-BCz fibers formed on glass substrates by exposing the spin-coated films to THF vapor for 16 h with different vapor pressures. The distances between the sample position and the solvent liquid surface are (A) 0.6, (B) 2.6, (C) 3, (D) 3.8, (E) 5.8, and (F) 7.4 cm. The inset in each image is the electron diffraction (ED) pattern of the selected area.

It indicates that H1-BCz has a good film-forming property and is suitable for use as an emissive material in an organic electro-luminescent device.²⁷

When the amorphous film is exposed to THF vapor, lots of holes and a few bundles of small fibers appear among the smooth film (Figure 5B, C), which means that both nucleation and dewetting have taken place. More fibers originate from the bundles and grow longer and thicker. As fibers grow, they branch off into new ones. The discontinuous dots near the fiber disappear, and the substrate is completely naked, which means that the substance of H1-BCz is consumed as the fiber grows (Figure 5D–H). The fibers grow to the area where the substance of H1-BCz is available. If there is a sufficient supply of the substance, the fibers grow straight. If there is a less than sufficient supply of the substance and the direction of the area of the substance departs from the long-axis exciting fiber, the fiber bends. At last, the fiber stops growing when the supply of the substance is stopped (Figure 5I). The acquired self-assembly morphology is similar to the morphology in Figure 2B. From the observed growth process of the fibers above, we can see that the growth process of the fibers is also influenced by the dewetting process of the thin films.

The change in the surface morphology of the film during the self-assembly process was further investigated by AFM. Figure 6 A and C shows that the growth front of the fiber goes deep into the amorphous film, and the film dewets back to the direction of the fiber growth from the substrate, but the situations will be different for the two fibers in Figure 6A. At the front of the right fiber, the dewetting has already taken place at the vicinal area, and the fiber stops growing for lack of substance. For the left fiber, the fiber front has intruded the film, and the fiber will continue to grow for the sufficient supply of the substance. It is believed that the substance will be consumed as the fiber grows and the length will eventually be different for the two fibers. The growth of the fiber may induce dewetting of the film, which is similar to the crystallization-induced dewetting process in thin polymer films.³⁶

Figure 6B shows that lots of small holes formed among the reserved films where the size of the dewetting hole is not so obvious. It may be the nucleation process of dewetting. In the area where dewetting has taken place, there is a much thinner film left, and among the film, there are some holes. The thicknesses of the holes are all ~ 1.58 nm (Figure 6E). From the dewetting phenomenon, the left layer may be a monolayer of the H1-BCz molecules.³⁷ From the growth front of the fiber after growing, we found that all the substance near the fibers is consumed (Figure 6F). From the AFM height image (Figure 6G) and the height profile (Figure 6H) across the line in Figure 6G, we can see that the thickness of the crystal is integer multiples of the thickness of the monolayer, and the thickness of the monolayer is ~ 1.6 nm. The front of the crystal displays up to 8 monolayers.

3.3. The Overlapping Layer Growth of H1-BCz Self-Assembly. The self-assembly of the H1-BCz fibers can take place on other substrates through THF vapor annealing, including glass, SiO_x , mica, quartz, ITO, and PEDOT: PSS. The self-assembly morphology is similar on different substrates, from single fibers at high vapor pressure to spherulites with crowded packing fibers at low vapor pressure. It indicates that the self-assembly of H1-BCz by solvent vapor annealing is general.

The UV-vis absorption and PL spectra for H1-BCz solution and amorphous and crystalline films are shown in Figure 7A. The maximum absorption peak for H1-BCz solution at 240 nm split into two peaks for amorphous and crystalline films. This may be due to the different vibronic modes of H1-BCz in solid films.³⁸ The abnormal blue shift of the PL spectrum for the crystalline film may be due to the nonhomocentric way of the dendrimer molecules' packing.³⁹ The shoulder peaks at 370 and 420 nm of PL spectra from a crystalline film on quartz substrate show that more adjacent carbazole groups forming partial or total eclipse excimers with benzene rings overlap in crystalline films.⁴⁰ The GIXD pattern of the self-assembled film on the SiO_x substrate in Figure 7B shows a strong reflection at $2\theta = 5.6^\circ$,

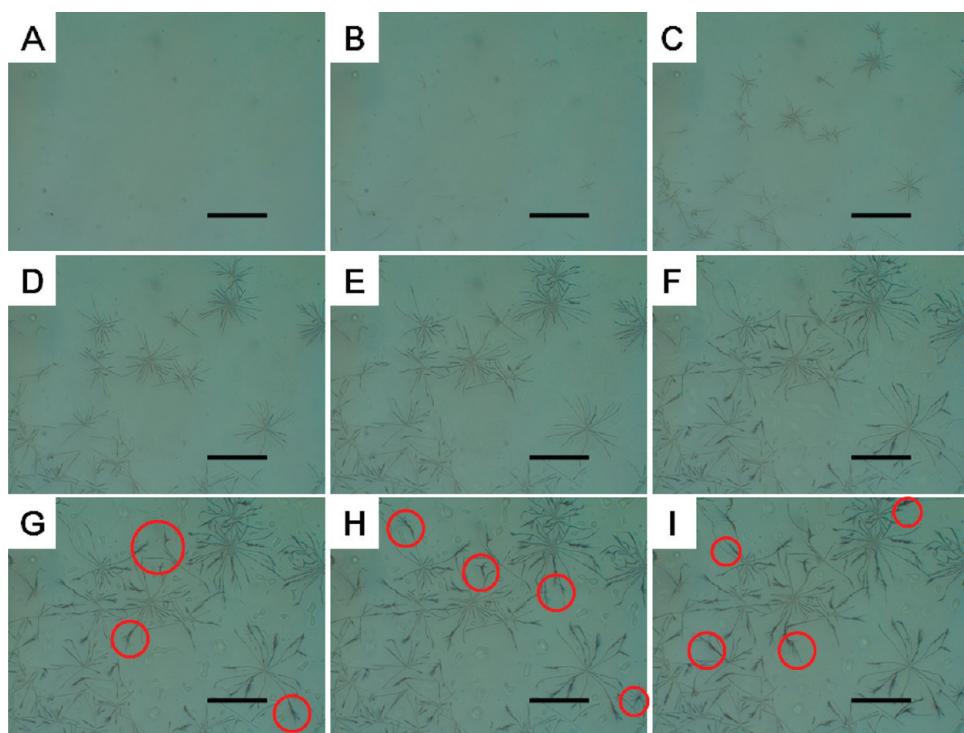


Figure 5. In situ observation of the self-assemble process. A, B, C, D, E, F, G, H, I are the snapshots from real-time optical microscopy taken at 0, 6, 7, 8, 9, 11, 15, 30, and 60 min, respectively, when the spin-coated film on glass substrates is exposed to the THF vapor. The selected areas are the newly grown fibers relative to the images of the last time scale. The sample is 1.6 cm higher than the solvent liquid surface, and the volume of the preadded solvent is 0.05 mL. The scale bar in each image is 500 μ m.

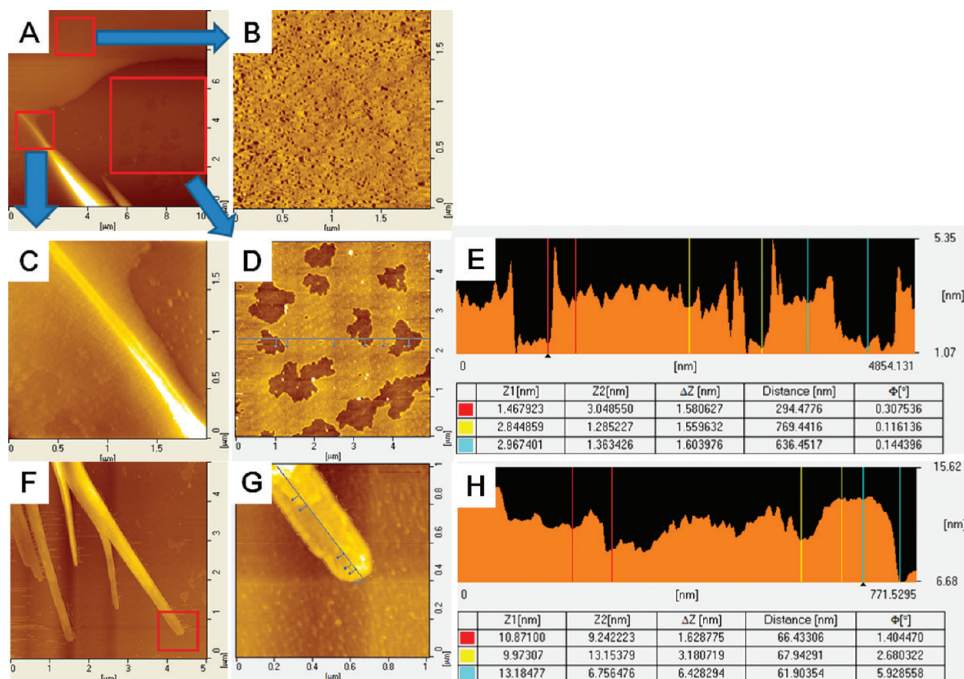


Figure 6. AFM height images of the fiber growth front on glass substrates (A) during the fiber growing and (F) after the fiber growth process. The sample was exposing to THF vapor for 8 min in a container with preadded 0.05 mL of THF. The sample position is 1.6 cm higher than the solvent liquid surface. B–D are the magnified AFM images of the selected areas in A. G is the magnified AFM height image of the selected area in F. E and H are the profiles across the line in D and G, respectively.

indicating a d spacing of 1.58 nm. This value corresponds to the thickness of the left monomolecular layer after dewetting and

the average layer thickness of the fiber growth front measured by AFM.

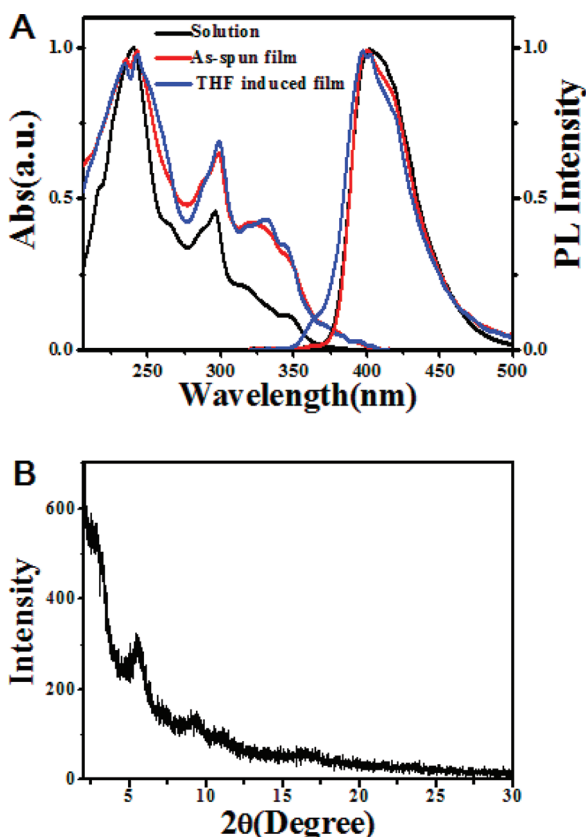


Figure 7. (A) UV-vis absorption spectra and PL spectra of H1-BCz in dilute CH_2Cl_2 solution (black line), amorphous film (red line), and crystalline film (blue line). The concentration of the solution is 1×10^{-5} M. The amorphous film is obtained by spin-coating a 10 mg/mL H1-BCz solution from chlorobenzene on quartz substrates. The crystalline film is fabricated by exposing the amorphous film on quartz substrate in THF vapor for 16 h where the sample is 7.4 cm higher than the solvent surface. (B) GIXD patterns of crystalline H1-BCz film from self-assembled spherulites on a silicon substrate by exposing the as-spun film in THF vapor for 16 h with a distance of 7.4 cm between sample and solvent surface.

On the basis of the measurement above, we may propose the proper mechanism of H1-BCz self-assembly process by solvent vapor annealing. At first, THF molecules absorb in the amorphous H1-BCz film, and the H1-BCz molecules partially dissolve in THF and have enough mobility. Second, the dissolved H1-BCz molecules rearrange to nucleate and grow into crystals. During this step, the $\pi-\pi$ stacking interactions among the phenyl-carbazole core and the carbazole dendrons may be the vital force. H1-BCz molecules form into a 2D lamellar structure first, and then the lamellar structures overlap to form 3D crystals. During the self-assembly process, the molecule-molecule and molecule-solvent interactions, such as $\pi-\pi$ stacking and van der Waals interactions, may be the main force to drive the molecules to rearrange and crystallize.^{30,41} The properties of substrates have little influence on the self-assembly behavior of H1-BCz dendrimer.

4. CONCLUSIONS

In summary, we have demonstrated the self-assembly of carbazole-based dendrimer H1-BCz and variation of the morphology from single fibers to spherulites by changing the vapor

pressure of the THF solvent. Large-size fibers with high molecular ordering are formed under high vapor pressure. Spherulites with different sizes are obtained when the vapor pressure is low. The different morphologies of the self-assembled fibers depend on the nucleation and growth processes, which are influenced by the different dewetting processes of the thin film under different vapor pressures. The H1-BCz crystal consists of an oriented layer-by-layer lamellar structure. The $\pi-\pi$ interactions and van der Waals interactions among the molecules and solvent may be the main force driving the self-assembly of H1-BCz. The properties of the substrates have little influence on the self-assembly behavior of H1-BCz. The result also shows the importance of removal of the solvent for the morphology stability of the amorphous films in organic electroluminescent devices.

■ AUTHOR INFORMATION

Corresponding Author

*Phone: 86-431-85262175. Fax: 86-431-85262126. E-mail: ychan@ciac.jl.cn.

■ ACKNOWLEDGMENT

This work was financially supported by the National Natural Science Foundation of China (20621401, 20834005, 51073151) and the National Basic Research Program of China (973 Program-2009CB930603).

■ REFERENCES

- (1) Bosman, A. W.; Janssen, H. M.; Meijer, E. W. *Chem. Rev.* **1999**, *99*, 1665–1688.
- (2) Rosen, B. M.; Wilson, C. J.; Wilson, D. A.; Peterca, M.; Imam, M. R.; Percec, V. *Chem. Rev.* **2009**, *109*, 6275–6540.
- (3) Astruc, D.; Boisselier, E.; Ornelas, C. *Chem. Rev.* **2010**, *110*, 1857–1959.
- (4) Lo, S.-C.; Burn, P. L. *Chem. Rev.* **2007**, *107*, 1097–1116.
- (5) Vogtle, F.; Gestermann, S.; Hesse, R.; Schwierz, H.; Windisch, B. *Prog. Polym. Sci.* **2000**, *25*, 987–1041.
- (6) Shetty, A. S.; Zhang, J. S.; Moore, J. S. *J. Am. Chem. Soc.* **1996**, *118*, 1019–1027.
- (7) Moore, J. S. *Acc. Chem. Res.* **1997**, *30*, 402–413.
- (8) Berresheim, A. J.; Muller, M.; Mullen, K. *Chem. Rev.* **1999**, *99*, 1747–1785.
- (9) Loi, S.; Butt, H. J.; Hampel, C.; Bauer, R.; Wiesler, U. M.; Mullen, K. *Langmuir* **2002**, *18*, 2398–2405.
- (10) Liu, D. J.; De Feyter, S.; Grim, P. C. M.; Vosch, T.; Grebel-Koehler, D.; Wiesler, U. M.; Berresheim, A. J.; Mullen, K.; De Schryver, F. C. *Langmuir* **2002**, *18*, 8223–8230.
- (11) Liu, D. J.; De Feyter, S.; Cotlet, M.; Wiesler, U. M.; Weil, T.; Herrmann, A.; Mullen, K.; De Schryver, F. C. *Macromolecules* **2003**, *36*, 8489–8498.
- (12) Xia, C. J.; Fan, X. W.; Locklin, J.; Advincula, R. C. *Org. Lett.* **2002**, *4*, 2067–2070.
- (13) Xia, C. J.; Fan, X. W.; Locklin, J.; Advincula, R. C.; Gies, A.; Nonidez, W. *J. Am. Chem. Soc.* **2004**, *126*, 8735–8743.
- (14) Morin, J. F.; Leclerc, M.; Ades, D.; Siove, A. *Macromol. Rapid Commun.* **2005**, *26*, 761–778.
- (15) Thomas, K. R. J.; Lin, J. T.; Tao, Y. T.; Ko, C. W. *J. Am. Chem. Soc.* **2001**, *123*, 9404–9411.
- (16) Kido, J.; Hongawa, K.; Okuyama, K.; Nagai, K. *Appl. Phys. Lett.* **1993**, *63*, 2627–2629.
- (17) Grazulevicius, J. V.; Strohriegl, P.; Pieliowski, J.; Pieliowski, K. *Prog. Polym. Sci.* **2003**, *28*, 1297–1353.
- (18) Drolet, N.; Morin, J. F.; Leclerc, N.; Wakim, S.; Tao, Y.; Leclerc, M. *Adv. Funct. Mater.* **2005**, *15*, 1671–1682.

- (19) Song, Y. B.; Di, C. A.; Wei, Z. M.; Zhao, T. Y.; Xu, W.; Liu, Y. Q.; Zhang, D. Q.; Zhu, D. B. *Chem.—Eur. J.* **2008**, *14*, 4731–4740.
- (20) Wu, Y. L.; Li, Y. N.; Gardner, S.; Ong, B. S. *J. Am. Chem. Soc.* **2005**, *127*, 614–618.
- (21) Guo, Y. L.; Zhao, H. P.; Yu, G.; Di, C. A.; Liu, W.; Jiang, S. D.; Yan, S. K.; Wang, C. R.; Zhang, H. L.; Sun, X. N.; Tao, X.; Liu, Y. Q. *Adv. Mater.* **2008**, *20*, 4835–4839.
- (22) Ong, B. S.; Li, Y. N.; Wu, Y. L. *Macromolecules* **2006**, *39*, 6521–6527.
- (23) Wakim, S.; Blouin, N.; Gingras, E.; Tao, Y.; Leclerc, M. *Macromol. Rapid Commun.* **2007**, *28*, 1798–1803.
- (24) Ding, J. Q.; Gao, J.; Cheng, Y. X.; Xie, Z. Y.; Wang, L. X.; Ma, D. G.; Jing, X. B.; Wang, F. S. *Adv. Funct. Mater.* **2006**, *16*, 575–581.
- (25) Ding, J. Q.; Lu, J. H.; Cheng, Y. X.; Xie, Z. Y.; Wang, L. X.; Jing, X. B.; Wang, F. S. *Adv. Funct. Mater.* **2008**, *18*, 2754–2762.
- (26) Ding, J. Q.; Wang, B.; Yue, Z. Y.; Yao, B.; Xie, Z. Y.; Cheng, Y. X.; Wang, L. X.; Jing, X. B.; Wang, F. S. *Angew. Chem., Int. Ed.* **2009**, *48*, 6664–6666.
- (27) Ding, J. Q.; Zhang, B. H.; Lu, J. H.; Xie, Z. Y.; Wang, L. X.; Jing, X. B.; Wang, F. S. *Adv. Mater.* **2009**, *21*, 4983–4986.
- (28) Albrecht, K.; Yamamoto, K. *J. Am. Chem. Soc.* **2009**, *131*, 2244–2251.
- (29) Lu, G. H.; Li, L. G.; Yang, X. N. *Adv. Mater.* **2007**, *19*, 3594–3598.
- (30) De Luca, G.; Liscio, A.; Maccagnani, P.; Nolde, F.; Palermo, V.; Mullen, K.; Samori, P. *Adv. Funct. Mater.* **2007**, *17*, 3791–3798.
- (31) Lee, W. H.; Kim, D. H.; Cho, J. H.; Jang, Y.; Lim, J. A.; Kwak, D.; Cho, K. *Appl. Phys. Lett.* **2007**, *91* (092105), 1–3.
- (32) Lee, W. H.; Lim, J. A.; Kwak, D.; Cho, J. H.; Lee, H. S.; Choi, H. H.; Cho, K. *Adv. Mater.* **2009**, *21*, 4243–4248.
- (33) Lu, G.; Li, L.; Yang, X. *Small* **2008**, *4*, 601–606.
- (34) Crossland, E. J. W.; Rahimi, K.; Reiter, G.; Steiner, U.; Ludwigs, S. *Adv. Funct. Mater.* **2011**, *21*, 518–524.
- (35) Granasy, L.; Pusztai, T.; Tegze, G.; Warren, J. A.; Douglas, J. F. *Phys. Rev. E* **2005**, *72* (011605), 1–15.
- (36) Okerberg, B. C.; Berry, B. C.; Garvey, T. R.; Douglas, J. F.; Karim, A.; Soles, C. L. *Soft Matter* **2009**, *5*, 562–567.
- (37) Shen, X. Y.; Ho, C. M.; Wong, T. S. *J. Phys. Chem. B* **2010**, *114*, 5269–5274.
- (38) Sun, Y. M.; Xiao, K.; Liu, Y. Q.; Wang, J. L.; Pei, J.; Yu, G.; Zhu, D. B. *Adv. Funct. Mater.* **2005**, *15*, 818–822.
- (39) Zhao, Z. J.; Li, J. H.; Chen, X. P.; Lu, P.; Yang, Y. *Org. Lett.* **2008**, *10*, 3041–3044.
- (40) Chung, P. S.; Holloway, P. H. *J. Appl. Polym. Sci.* **2009**, *114*, 1–9.
- (41) Palermo, V.; Samori, P. *Angew. Chem., Int. Ed.* **2007**, *46*, 4428–4432.